1521-0111/12/8204-711–718$25.00
MOLECULAR PHARMACOLOGY
Vol. 82, No. 4
78683/3796001
Mol Pharmacol 82:711–718, 2012

Efficient Binding of 4/7 α-Conotoxins to Nicotinic α4β2 Receptors Is Prevented by Arg185 and Pro195 in the α4 Subunit[S]

Mirko Beissner, Sébastien Dutertre, Rudolf Schemm, Timm Danker, Annett Sporning, Helmut Grubmüller, and Annette Nicke

Department of Neurochemistry, Max Planck Institute for Brain Research, Frankfurt, Germany (M.B., A.N.); Institute for Molecular Bioscience, University of Queensland, Brisbane, Queensland, Australia (S.D.); Department of Theoretical and Computational Biophysics, Max Planck Institute for Biophysical Chemistry, Göttingen, Germany (R.S., H.G.); NMI Technologie Transfer GmbH, Reutlingen, Germany (T.D.); and Department of Molecular Biology of Neuronal Signals, Max Planck Institute for Experimental Medicine, Göttingen, Germany (A.S., A.N.)

Received March 17, 2012; accepted July 16, 2012

ABSTRACT

α-Conotoxins are subtype-selective nicotinic acetylcholine receptor (nAChR) antagonists. Although potent α3β2 nAChR-selective α-conotoxins have been identified, currently characterized α-conotoxins show no or only weak affinity for α4β2 nAChRs, which are, besides α7 receptors, the most abundant nAChRs in the mammalian brain. To identify the determinants responsible for this difference, we substituted selected amino acid residues in the ligand-binding domain of the α4 subunit by the corresponding residues in the α3 subunit. Two-electrode voltage clamp analysis of these mutants revealed increased affinity of α-conotoxins MII, TxIA, and [A10L]TxIA at the α4(R185I)β2 receptor. Conversely, α-conotoxin potency was reduced at the reverse α3(I186R)β2 mutant. Replacement of α4Arg185 by alanine, glutamate, and lysine demonstrated that a positive charge in this position prevents α-conotoxin binding. Combination of the R185I mutation with a P195Q mutation outside the binding site but in loop C completely transferred high α-conotoxin potency to the α4β2 receptor. Molecular dynamics simulations of homology models with docked α-conotoxin indicate that these residues control access to the α-conotoxin binding site.

Introduction

Neuronal nicotinic acetylcholine receptors (nAChRs) constitute a diverse family of pentameric ion channels that are formed by variable assembly from at least eight α and three β subunits (α2–α6, α7, α9, α10, and β2–β4). The α2, α3, α4, and α6 subunits require coexpression of at least one β (β2 or β4) subunit to form functional channels. The ACh binding site has been located at the interface between an α subunit (+face) and an adjacent β subunit (−face), or, in the case of the α7, α9, and α10 subunits, another α subunit (−face). The "structural" α5 and β3 subunits seem to be unable to form functional channels in any pairwise combination but contribute to the diversity of pentameric αβ combinations in channels with three or four different subunits (Gotti et al., 2009).

The nicotinic α4β2* subtype (* denotes the possible presence of additional subunits) is the most abundant heteromeric nicotinic receptor in the brain. It plays a role in cognitive processes and represents a therapeutic target for smoking cessation as well as for the treatment of pain and a variety of neurological disorders such as Alzheimer's and Parkinson's diseases, depression, and attention deficit disorders (Taly et al., 2009). α-Conotoxins, a family of small disulfide peptides isolated from the venom of predatory marine snails, are highly selective nAChR antagonists that bind at the intersubunit agonist binding site and thereby discriminate between closely related nAChR subtypes. They have proven to be useful pharmacological tools to localize nAChR subtypes and to investigate their specific subunit composition and physiological functions (Nicke et al., 2004). The 4/7 α-conotoxins represent the largest α-conotoxin subfamily. Most of the identified 4/7 α-conotoxins target α7 and/or

This work was supported by the Deutsche Forschungsgemeinschaft [Grants NI 592/3 and 592/5].
M.B., S.D., and R.S. contributed equally to this work.
Article, publication date, and citation information can be found at http://molpharm.aspetjournals.org.
http://dx.doi.org/10.1124/mol.112.078683.
[S] The online version of this article (available at http://molpharm.aspetjournals.org) contains supplemental material.

ABBREVIATIONS: ACh, acetylcholine; nAChR, nicotinic acetylcholine receptor; AChBP, acetylcholine binding protein; MD, molecular dynamics; wt, wild-type; TEVC, two-electrode voltage clamp.

$\alpha3\beta2$* nAChRs with low nanomolar potency. Equally potent 4/7 α-conotoxins with selectivity for the $\alpha6\beta2$ receptor (which is closely related to the $\alpha3\beta2$ subtype) have been isolated from crude venom or have been generated by modification of the $\alpha3\beta2$- and $\alpha6\beta2$-selective α-conotoxin MII (Nicke et al., 2004; Azam and McIntosh, 2009). So far, no conotoxin that selectively targets $\alpha4\beta2$ nAChRs has been identified, and only a few α-conotoxins, MII (Cartier et al., 1996), GID (Nicke et al., 2003), GIC (McIntosh et al., 2002), and AnIB (Loughnan et al., 2004), have been shown to block this receptor at all, although at high nanomolar or micromolar concentrations.

Given the abundance of $\alpha4\beta2$* receptors in the brain and their importance as drug targets, potent and specific pharmacological tools for this receptor are needed. Here we show that an arginine residue in position 185 and a proline residue in position 195 of the $\alpha4$ subunit prevent efficient α-conotoxin binding. Our data provide molecular determinants of subtype selectivity and thus represent a basis for the design of optimized α-conotoxins with tailored subtype selectivity.

Materials and Methods

Homology Modeling and Molecular Dynamics Simulations. The dimeric homology model of the ligand-binding domain of the $\alpha4\beta2$ nAChRs was based on the muscle-type nAChR (Unwin, 2005). This model was generated with Modeler9v8-1 (Sali and Blundell, 1993) using two α subunits of the refined electron microscopic structure of the *Torpedo marmorata* nAChR polypeptide chains (Protein Data Bank code 2BG9). These show a considerably higher homology to the $\alpha4$ and $\beta2$ nAChR subunits than that of the AChBP. Although the structural assignment might be critical because of the resolution of only 4 Å of 2BG9, a recently published structure of the Glu-gated chloride channel GluCl (3.3 Å; Protein Data Bank code 3RIF) (Hibbs and Gouaux, 2011) and the common alignment of the loop C region support its reliability. For a comparison of this model with a previously generated AChBP-based model in terms of structural changes of loop C (root mean square), see Supplemental Fig. 2.

Because we intended to measure binding energies of conotoxins, which correlate with their ability to inhibit AChRs and not gating movements, we decided to use a dimeric model for docking and molecular dynamics (MD) studies instead of using a full receptor or ligand-binding domain model. This model was also more feasible in terms of simulation times needed for statistical analysis. All MD simulations were performed using Gromacs (versions 4.0.7 and 4.5.5) (Hess et al., 2008) and the amber03 force field (Duan et al., 2003). Dimeric wild-type and mutant $\alpha4\beta2$ ligand binding domains with α-conotoxin [A10L]TxIA were generated with the capping groups ace and nme (Sybyl 8.0.1; Tripos, St. Louis, MO). The proteins were placed in a rectangular box filled with tip4p water (Mahoney and Jorgensen, 2000) and Na^+ and Cl^- ions (0.15 M) and, after energy minimization, were subjected to 50-ns MD runs whereby position restraints of 10 kJ/(mol · nm^2) were set on the protein atoms (without H) except for loop C (Tyr182–Ile197) and the conotoxin. From the resulting trajectories, distances and binding energies (sum of short-range Coulomb and Lennard-Jones energies) of the α-conotoxin to the $\alpha4$ and $\beta2$ subunits, respectively, were calculated. For this purpose, from each trajectory 20,000 frames (10–50 ns) were used for analysis. The first 10 ns from each trajectory were discarded to minimize equilibration effects. For each value, 8 to 10 trajectories were generated, and distances and interaction energies were averaged (Fig. 5). To determine the significance of the overall trend for stronger binding enthalpies for $0 < 1 < 2 < 3$, a Bayesian analysis (see supplemental data) for linear fit functions $y = m \cdot x + b$ was performed with $x = [0, 1, 2, 3]$ for [wt, P195Q, R185I, P195Q/R185I], respectively, assuming an unbiased a priori distribution for the slope m and the offset b. For the resulting a posteriori probability distribution $p(m)$, integrated over all offsets, a probability of 0.9986 is found for negative m, implying a significance level of 0.14%.

Peptide Sources. α-MII was obtained from Tocris Bioscience (Ellisville, MO). α-TxIA and α-[A10L]TxIA were synthesized using Boc chemistry with in situ neutralization protocols as described previously (Dutertre et al., 2007).

Electrophysiological Measurements. nAChR cDNAs were provided by J. Patrick (Baylor College of Medicine, Houston, TX) and subcloned into the oocyte expression vector pNKS2. Site-directed mutagenesis was performed with the QuikChange Mutagenesis Kit (Stratagene, La Jolla, CA). Primer synthesis and sequencing was performed by MWG Biotech AG (Ebersberg, Germany). cRNA was synthesized with the SP6 mMessage mMachine Kit (Ambion, Austin, TX), and *Xenopus laevis* (Nasco International, Fort Atkinson, WI) oocytes were injected with 50-nl aliquots of cRNA (0.5 mg/ml), either manually or using the Roboinject robot (MCS, Reutlingen, Germany). nAChR subunits were mixed in the ratios 1:1 ($\alpha3/\beta2$) or 5:1 ($\alpha4/\beta2$).

Antagonist dose-response curves were measured as described previously (Dutertre et al., 2005) in ND96 (96 mM NaCl, 2 mM KCl, 1 mM $CaCl_2$, 1 mM $MgCl_2$, and 5 mM HEPES at pH 7.4). In brief, current responses to acetylcholine were recorded at −70 mV using a Turbo Tec 05X Amplifier (NPI Electronic, Tamm, Germany) and CellWorks software. A standard concentration of 100 μM ACh was used to keep the data comparable with previous studies. However, comparison of the inhibition of the $\alpha3\beta2$ subtype by 3 nM [A10L]TxIA at 30, 100, and 300 μM (approximately EC_{50} for wild-type $\alpha3\beta2$) ACh showed no significant differences in the toxin effect, suggesting that the ACh concentration is not critical under the conditions described (preapplication of toxin). A fast and reproducible solution exchange (<300 ms) was achieved with a 50-μl funnel-shaped oocyte chamber combined with a fast solution flow (~150 μl/s) fed through a custom-made manifold mounted immediately above the oocyte. Agonist pulses were applied for 2 s at 4-min intervals. Peptides were applied for 3 min in a static bath. IC_{50} values were calculated from a nonlinear fit of the Hill equation to the data (Prism version 4.0; GraphPad Software, Inc., San Diego, CA). Data are presented as means ± S.E. from at least four experiments.

Agonist dose-response curves for ACh were recorded in Ca^{2+}-free buffer (96 mM NaCl, 2 mM KCl, 1 mM MgSO4, and 5 mM HEPES, pH 7.4), supplemented with 0.5 μM atropine, using the Roboocyte platform (MCS) (Pehl et al., 2004; Leisgen et al., 2007) or the conventional TEVC setup described above. Oocytes were clamped at −60 or −70 mV, and 2- or 3-s pulses of the indicated agonist concentrations were applied in alternation with a 200 (Roboocyte) or 300 μM reference concentration to account for receptor rundown. Current responses to ACh were calculated in relation to the reference pulses, and the normalized dose-response data were fitted to the four-parameter Hill equation using Prism. If the Hill coefficient could not be accurately determined, it was constrained to a range from 0 to 2.

Results

Generation and Functional Expression of Mutant $\alpha4\beta2$ nAChRs. The $\alpha4$ and $\alpha3$ nAChR subunits have 61.84% sequence identity in their ligand-binding domain. From the sequence alignment of these two sequences (Fig. 1), we selected four amino acid residues located in the proposed conotoxin binding site that differed between the $\alpha4$ subunit and the $\alpha3$ subunit. With use of site-directed mutagenesis, these $\alpha4$ residues were replaced with the respective $\alpha3$ residues T147S, R185I, E188N, and A191E. To confirm that the mutations do not markedly alter the functional properties of the receptors, wt and mutant $\alpha4$ subunits were coexpressed with the $\beta2$ subunits in *X. laevis* oocytes and

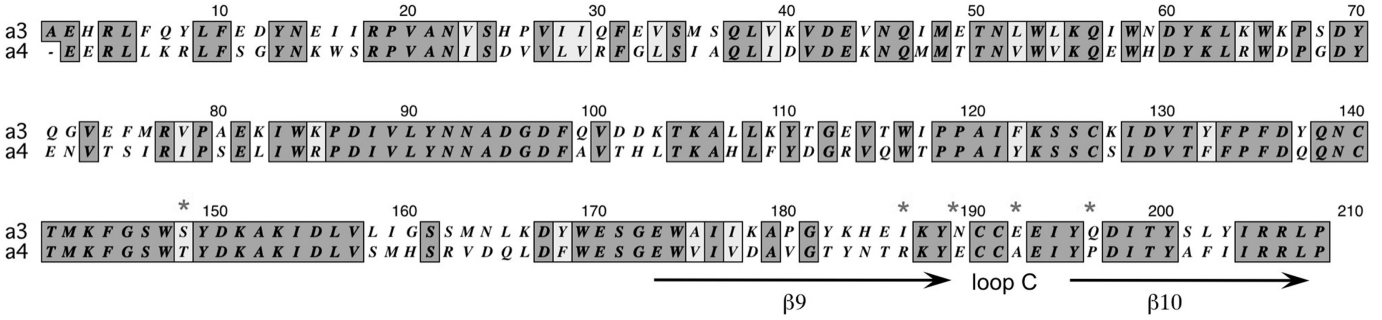

Fig. 1. Sequence alignment. Rat α4 and α3 nAChR subunits have 61.84% sequence identity in their ligand-binding domain. Asterisks indicate the position of residues mutated in this study.

dose-response curves for ACh were recorded using the Roboocyte automated two-electrode voltage clamp system (Fig. 2). This automated screen revealed that all single point mutants were functionally expressed, and their EC_{50} values for ACh were of the same order of magnitude as that of the wt receptor (Table 1).

The α4R185I Mutation Enables Efficient Binding of α-Conotoxins MII, TxIA, and [A10L]TxIA to the α4β2 Receptor. α-Conotoxin MII blocks heterologously expressed α3β2 and α6β2* nAChRs with low nanomolar potency (IC_{50} = 0.5–8 and 0.4 nM, respectively) (Cartier et al., 1996; Harvey et al., 1997; Kaiser et al., 1998; Dowell et al., 2003; McIntosh et al., 2004). Because it also blocks α4β2 nAChRs at approximately 100- to 1000-fold higher concentrations (IC_{50} = 430–550 nM) (Cartier et al., 1996), we initially determined dose-response relationships of α-conotoxin MII on wt and mutant α4β2 nAChRs to test whether any of the mutations in the α4 subunit improved its affinity. As shown in Fig. 3A and Table 2, the α4R185I exchange caused a more than 10-fold decrease in the IC_{50} value (193 nM) compared with that for the wt α4β2 nAChR (3293 nM), whereas no other mutations significantly altered the potency of MII. To examine whether these findings were specific for α-conotoxin MII, we next investigated the dose-response relationships of α-conotoxins TxIA and [A10L]TxIA. As determined previously (Dutertre et al., 2007), TxIA and [A10L]TxIA have potency similar to that of MII on α3β2 nAChRs (IC_{50} = 2 and 3.6 nM, respectively); however, in contrast to MII, they also block homomeric α7 nAChR with IC_{50} values of 390 and 39 nM, respectively, and show no affinity for the α4β2 receptor at concentrations up to 10 μM (Dutertre et al., 2007). Both analogs have comparably little sequence identity with MII apart from the residues that are generally conserved in most 4/7 α-conotoxins, namely the four cysteine residues, G1, and P6 (Table 3). As seen with MII, no significant improvement in affinity resulted from the T147S, E188N, and A191E mutations in the α4 subunit, whereas the effect of the R185I mutation was even stronger than that for MII with a more than 1000-fold affinity increase, which made TxIA a potent blocker (IC_{50} = 18 nM) at this mutant (Fig. 3B). Likewise, the [A10L]TxIA-analog was rendered into an efficient antagonist (IC_{50} = 123 nM) at the α4(R185I)β2 mutant (Fig. 3D).

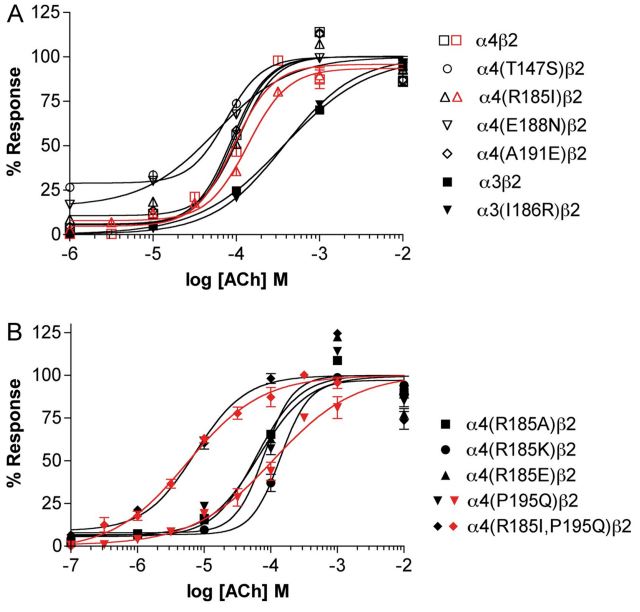

Fig. 2. Agonist dose-response curves for ACh. The indicated wt and mutant α3 and α4 subunits were coexpressed with β2 subunits in *X. laevis* oocytes. Responses to ACh were measured at −60 mV with the Roboocyte system or at −70 mV with a conventional TEVC setup (red lines and symbols, control experiments for the most critical mutants in this study). Dose-response curves for wt and mutant α3β2 and α4β2 receptors (A) and different α4β2 mutants (B) are shown.

The α3I186R Mutation Impairs Binding of α-Conotoxins MII, TxIA, and [A10L]TxIA to the α3β2 Receptor. Arg185 lies in a stretch of 15 amino acids (174–188) in the β9 strand preceding the critical cysteine pair that forms a vicinal disulfide bridge at the tip of loop C, which covers the intersubunit binding site (Fig. 1). These residues are highly variable between the α3 and α4 subunits, which might result in different backbone conformations of loop C and consequently generally different dimensions or accessibility of the conotoxin binding sites. However, our results with MII demonstrate that the α4β2 binding site can principally accommodate α-conotoxins, but that Arg185 might specifically clash with one or more residues in the α-conotoxins and thus prevent or impair their high-affinity binding. To further investigate the specific role of the side chain in this position we replaced the equivalent isoleucine residue in the α3β2 receptor by an arginine residue. This I186R exchange in the α3 subunit caused a more than 10-fold decrease in the affinity of MII (IC_{50} = 58 nM) and a 30-fold decrease in the affinity of TxIA (IC_{50} = 60 nM) and [A10L]TxIA (IC_{50} = 77 nM). Thus, TxIA was slightly more potent at the α4(R185I)β2 receptor than at the α3(I186R)β2 receptor. These results are in agreement with our assumption that Arg185 specifically interacts with α-conotoxin binding.

TABLE 1

EC_{50} values for acetylcholine at wt and mutant $\alpha3\beta2$ and $\alpha4\beta2$ receptors obtained with the Roboocyte system

Hill coefficients were constrained between 0 and 2 in cases in which the coefficients obtained originally were unreliable (CI >4).

	EC_{50}	95% CI	Hill Slope
	μM		
$\alpha3\beta2$	369.6	302–453	0.9
$\alpha3$(I186R)$\beta2$	376.7	313–454	1.0
$\alpha4\beta2$	91.9/93.9[a]	76–111/76–117[a]	2.0/1.9[a]
$\alpha4$(T147S)$\beta2$	75.2	44–128	2.0
$\alpha4$(A191E)$\beta2$	87.3	67–113	2
$\alpha4$(E188N)$\beta2$	56.7	46–71	1.0
$\alpha4$(R185I)$\beta2$	108.9/138.0[a]	88–135/115–166[a]	2.0/1.8[a]
$\alpha4$(R185A)$\beta2$	61.4	45–84	1.3
$\alpha4$(R185K)$\beta2$	139.8	91–214	2.0
$\alpha4$(R185E)$\beta2$	80.3	52–125	2.0
$\alpha4$(P195Q)$\beta2$	66.5/110.5[a]	37–120/43–282[a]	1.2/0.7[a]
$\alpha4$(P195Q/R185I)$\beta2$	7.3/5.6[a]	3.2–16.4/3.6–8.7[a]	1.1/0.8[a]

CI, confidence interval.

[a] For comparison, entries represent values obtained in a conventional TEVC setup.

α-Conotoxin Binding to $\alpha4\beta2$ Receptors Is Prevented by a Positively Charged Residue in Position 185 of the $\alpha4$ Subunit. Next we exchanged Arg185 in the $\alpha4$ subunit by alanine, lysine, and glutamate to determine whether a positive charge is required to prevent α-conotoxin binding or whether this is due to a steric effect of the bulky arginine side chain. As shown in Fig. 3D, replacement of arginine by alanine or the negatively charged glutamate caused potency increases of [A10L]TxIA comparable with those for the substitution by isoleucine with IC_{50} values of 372 and 118 nM, respectively. In contrast, [A10L]TxIA was inactive at the $\alpha4$(R185K)$\beta2$ mutant. Together with the fact that the substitution by the negatively charged glutamate resulted in a 3-fold lower IC_{50} value than substitution by the small alanine, this suggests that a positive charge in position 185 of the α subunit prevents α-conotoxin binding.

An Additional $\alpha4$P195Q Mutation Completely Transfers Low Nanomolar Potency of [A10L]TxIA to the $\alpha4\beta2$ Receptor. The α-conotoxin potencies achieved at the $\alpha4$R185I$\beta2$ receptor are still in the medium to high (20–200 nM) nanomolar range. In contrast, low to subnanomolar potencies are usually achieved at $\alpha3\beta2$ and the closely related $\alpha6\beta2$ subtype or the homomeric $\alpha7$ subtype. On the basis of sequence alignment and homology modeling, we hypothesized that proline 195 could constitute the remaining obstacle (Fig. 1). Although it does not directly face the α-conotoxin binding site, it might disturb the binding by structurally altering loop C. Indeed, replacement of $\alpha4$Pro195 by the homologous glutamine residue found in the $\alpha3$ subunit rendered [A10L]TxIA active at this receptor (IC_{50} = 707 nM). In combination with the R185I substitution, the P195Q mutation caused an additional 40-fold increase in the potency of [A10L]TxIA and rendered this mutant $\alpha4\beta2$ receptor as sensitive (IC_{50} = 3.2 nM) to [A10L]TxIA as the $\alpha3\beta2$ subtype. Of interest, the R185I/P195Q double exchange also significantly increased the sensitivity to ACh as determined by both automated and conventional analysis of dose-response curves (Table 1; Fig. 2).

Probing the Binding Mode of [A10L]TxIA at the $\alpha4\beta2$ Receptor. We had previously identified several mutants in the $\beta2$ subunit that improve the efficiency of conotoxins with a long side chain in position 10 to block the $\alpha3\beta2$ receptor

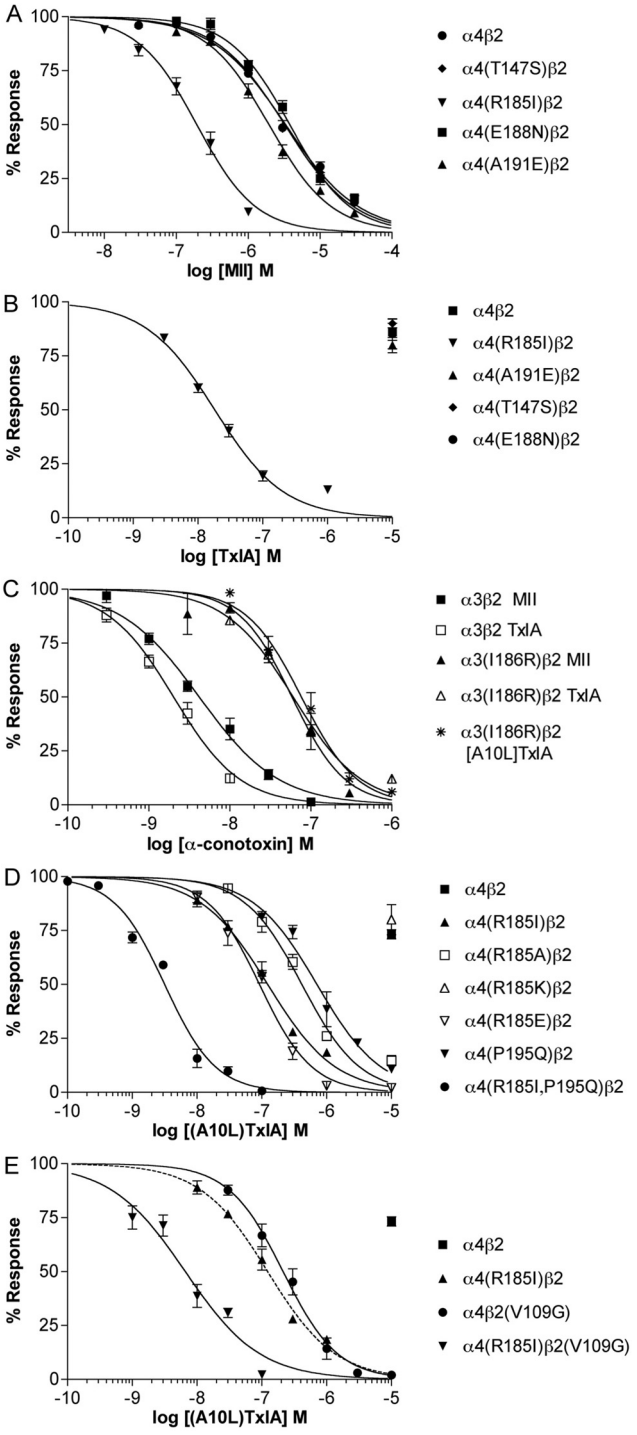

Fig. 3. Concentration-response analysis of α-conotoxins MI, TxIA, and [A10L]TxIA on wild type and mutant nAChRs. A to E, the subunit combinations indicated were expressed in *X. laevis* oocytes and analyzed by two-electrode voltage clamp. Responses to 2-s pulses of 100 μM ACh were recorded after a 3-min preincubation with the indicated toxin. IC_{50} values and Hill slopes are given in Table 2. Each point represents the average of at least four measurements. Error bars represent S.E. The dotted line in E shows the same data as in D.

(Dutertre et al., 2005). We deduced from these studies that the first loop of α-conotoxins (residues 4–7) faces toward the α-subunit, whereas the second loop (residues 9–15) interacts with the β subunit. This binding mode is in good agreement with cocrystallization studies of the acetylcholine-binding

TABLE 2

IC_{50} values and Hill coefficients for the α-conotoxins MII, TxIA, and [A10L]TxIA at wt and mutant α3β2 and α4β2 receptors

Values in parentheses represent 95% confidence intervals.

	MII		TxIA		[A10L]TxIA	
	IC_{50}	n_H	IC_{50}	n_H	IC_{50}	n_H
	nM		*nM*		*nM*	
α4β2	3293 (2855–3798)	−0.852				
α4(T147S)β2	3206 (2538–4050)	−0.903			N.D.	
α4(E188N)β2	3766 (3253–4361)	−1.03			N.D.	
α4(A191E)β2	1938 (1683–2233)	−0.996			N.D.	
α4(R185I)β2	192.8 (158–236)	−1.058	18.1 (15.2–21.6)	−0.813	123 (102–113)	−0.835
α4((R185A)β2	N.D.		N.D.		415 (333–515)	−0.980
α4(R185K)β2	N.D.		N.D.			
α4(R185E)β2	N.D.		N.D.		91.8 (74.8–113)	−1.079
α4β2(V109G)	N.D.		N.D.		213 (167–271)	−1.031
α4(R185I) β2(V109G)	N.D.		N.D.		6.6 (4.8–9.1)	−0.755
α4(P195Q)β2	N.D.		N.D.		707 (533–939)	−0.88
α4(R185I,P195) β2	N.D.		N.D.		3.2 (2.6–3.8)	−1.11
α3β2	4.2	−0.887	2 (1.68–2.43)	−1.062	2.0 (1.8–2.4)[a]	–
α3(I186R)β2	58.3 (45.1–75.5)	−1.327	60.4 (50.9–71.6)	−1.033	76.5 (58.9–99.3)	−1.261

n_H, Hill coefficient; N.D., not done.
[a] Data from Dutertre et al. (2007).

TABLE 3

Sequence comparison of the 4/7 α-conotoxins

Underlining indicates residues that are generally conserved. Two of 8 and 3 of 16 cysteine pairs form disulfide bridges.

	1111111 1234567890123456
MII	GCCSNPVCHLEHSNLC
TxIA	GCCSRPPCIANNPDLC
[A10L]TxIA	GCCSRPPCILNNPDLC
PnIA	GCCSLPPCAANNPDYC
EpI	GCCSDPRCNMNNPCYC
GID	IRDγCCSNPACRVNNOHVC

protein and was further refined in subsequent functional studies (Celie et al., 2005; Dutertre et al., 2007). To test whether a principally similar binding mode was preserved in the α4R185Iβ2 mutant, we combined in analogous experiments the α4R185I subunit with the previously identified β2V109G mutant (Dutertre et al., 2005). Combination of these subunits caused an additional potency increase of [A10L]TxIA that was at least 20-fold higher (IC_{50} = 6.6 nM) than that for each single mutation in combination with the respective wt subunit (IC_{50} = 123 and 213 nM, respectively) (Fig. 3E; Table 2). Because we had previously found that the β2V109G mutation causes a potency increase of α-conotoxins with a long side chain in position 10 in combination with both wt α3 and wt α4 subunits (Dutertre et al., 2005), we suggest that this interaction with the β2(V109G) subunit is preserved in a similar way if combined with the α4(R185I) subunit. Consequently, the binding mode should not be different from what we have determined for the α3β2 receptor (Dutertre et al., 2005) and the α4 subunit probably interacts with the N terminus of the α-conotoxin.

Computational Studies of α-Conotoxin Binding Mode at α4β2 Receptors. Next, we placed [A10L]TxIA in the binding pocket of a α4β2 homology model in the same position where it was cocrystallized with AChBP (Dutertre et al., 2007). However, this procedure failed to identify a direct interaction of α4Arg185 with any conotoxin residue or with the conotoxin backbone (Fig. 4A). We therefore performed docking studies on a homology model based on the refined structure of the *T. marmorata* nAChR (Unwin, 2005) α4 subunit (Fig. 4B). Remarkably, these docking simulations revealed an interaction of α4Arg185 with the arginine residue in position 5 of the conotoxins (Fig. 4B; Supplemental Figs. 1A and 2). In addition, MD simulations revealed a weaker binding of conotoxin [A10L]TxIA at the wt protein (Fig. 4, C–E). In contrast, the same MD simulations run with the R185I mutation allow the conotoxin to bind deeper in its binding pocket (Fig. 4, C and E). In addition, the P195Q substitution results in a greater flexibility of loop C, enabling a more peripheral position of the critical Arg185 residue that likewise allows a closer contact to the conotoxin (Figs. 4D and 5A). For the R185I/P195Q double mutation, both effects lead to further improved positioning of the conotoxin (Fig. 4E; Supplemental Fig. 1B). However, no significant correlation between distance and conotoxin binding enthalpies is seen (Fig. 5, A and B). For example, the conotoxin-β2 subunit distances remain between 1.5 and 1.6 nm, although the respective energies decrease, implying stronger binding. Apparently, the different binding enthalpies are not explained by the distances between [A10L]TxIA and the β2 subunit. We also investigated the involvement of the loop C-conotoxin interaction in the measured overall binding energies. However, the results for the different protein-conotoxin combinations (Supplemental Fig. 3) do not strictly correlate with the calculated binding energies (Fig. 5). Consequently, we cannot ascribe the conotoxin-protein interactions found to the respective conotoxin-loop C residue interactions solely. Likewise, single fluctuations of loop C residues seem to be independent of the actual mutation state (Supplemental Fig. 4). Nevertheless, analysis of structural changes (root mean square deviation) during MD to estimate the contributions of loops C to conotoxin binding showed that Arg185 has the largest influence on loop C conformation (Supplemental Fig. 2).

Although no significant binding enthalpy difference is seen for the P195Q mutation, the binding enthalpy is significantly stronger than that in the wt for both the R185I mutant and the P/R double mutant (Fig. 5B). Moreover, an overall trend to stronger binding enthalpies of [A10L]TxIA with wt < P195Q < R185I < P195Q/R185I is seen at a significance level of 5×10^{-4} (see supplemental data) and reflects the results obtained in functional experiments (Fig. 5B).

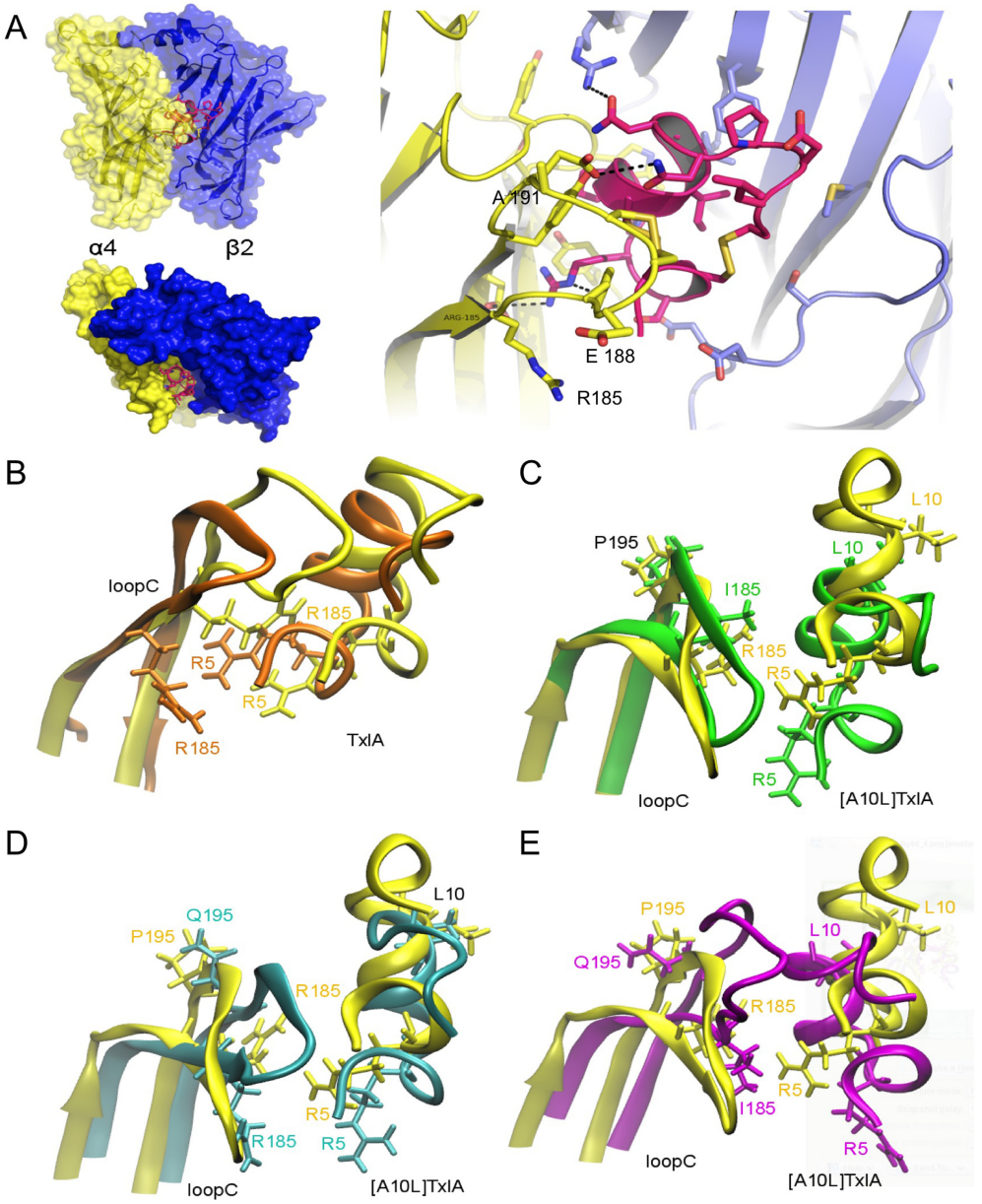

Fig. 4. Molecular simulations of conotoxin binding in wt and mutant $\alpha4\beta2$ homology models. A, position of TxIA in the binding site of $\alpha4\beta2$ on the basis of the cocrystal structure with AChBP, showing the absence of a steric clash between the conotoxin and receptor residues. The model of the $\alpha4\beta2$ receptor was generated using the AChBP bound to TxIA crystal structure as a template, as described previously (Dutertre et al., 2007). B, loops C of wt $\alpha4$ subunit models based on AChBP (orange) and *T. marmorata* nAChR (yellow) with the respective TxIA (starting structures). C, D, and E, loops C of wt (yellow), $\alpha4$(R185I)$\beta2$ (green), $\alpha4$(P195Q)$\beta2$ (cyan), and $\alpha4$(R185I, P195Q)$\beta2$ (magenta) receptor models based on the *T. marmorata* nAChR with the [A10L]TxIA conotoxin in minimized average structures.

Discussion

In this study, we have identified two amino acid residues, Arg185 and Pro195, in the $\alpha4$ nicotinic receptor subunit that, if replaced by the corresponding residues in the $\alpha3$ subunit, completely transferred the low nanomolar potency of α-conotoxin [A10L]TxIA to the $\alpha4\beta2$ subtype, which is otherwise insensitive to this toxin. Replacement of Arg185 by isoleucine resulted in a 10-fold (MII) up to at least 1000-fold (TxIA and [A10L]TxIA) enhanced potency of different 4/7 α-conotoxins at the $\alpha4\beta2$ receptor subtype. Replacement of the corresponding Ile186 residue in the $\alpha3$ subunit by an arginine residue reduced the potency of these conotoxins at the $\alpha3\beta2$ receptor more than 10-fold. These findings are in good agreement with previous studies that demonstrated the importance of these two residues (Harvey et al., 1997) for MII and PnIA binding to the $\alpha3\beta2$ receptor by replacing them with the homologous residues (K and P, respectively) from the conotoxin-insensitive $\alpha2$ subunit (Everhart et al., 2003). Here, we further demonstrate that replacement of $\alpha4$Arg185 by the smaller alanine or a negatively charged glutamate but not by a positively charged lysine enhanced affinity of the $\alpha4\beta2$ receptor for [A10L]TxIA. We conclude from these data that a positive charge in this position specifically prevents high-affinity binding of most conotoxins to the $\alpha4\beta2$ nicotinic receptor and thus represents a major determinant for subtype selectivity. Because arginine and lysine are both very bulky residues, a steric interaction rather than a charge effect of $\alpha4$Arg185 cannot be excluded and could explain the lack of activity of 4/7 α-conotoxins that carry a noncharged leucine residue in position 5 (such as PnIA and PnIB). In support of a charge effect, however, the α-conotoxins identified that show low activity at the $\alpha4\beta2$ receptor (MII, GID, GIC, and AnIB) have a neutral asparagine residue or an only partially protonated (at pH 7.4) histidine residue in this position.

The strong effect of the $\alpha4$(R185I/P195Q) double mutation on the EC_{50} value for ACh might indicate that the combina-

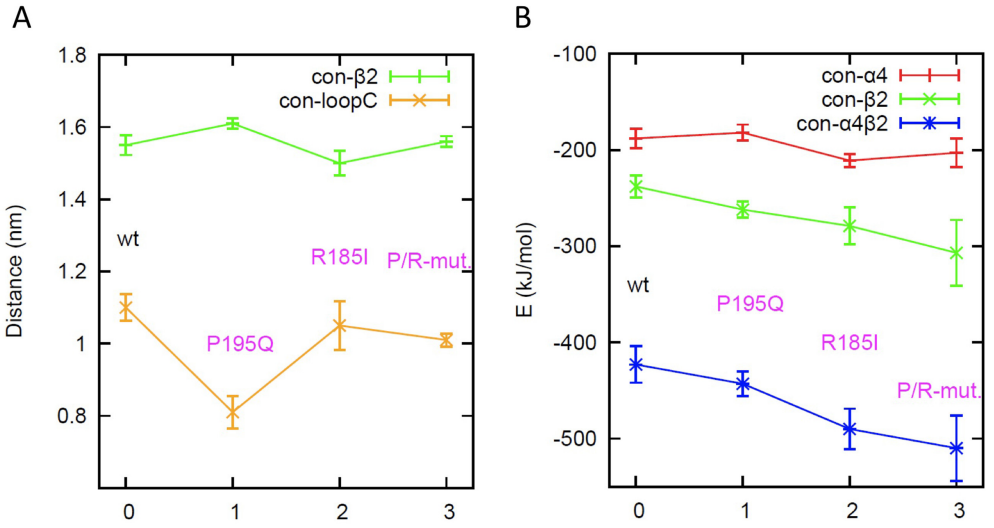

Fig. 5. Calculated average [A10L]TxIA α-conotoxin (con) distances and binding enthalpies. A, α-conotoxin distances to loop C [Arg(Ile)185–Tyr194] of α4 (orange) and to the β2 subunit (center of mass of backbone) (green). B, binding enthalpies (sum of short-range Coulomb + Lennard-Jones energies) for α-conotoxin [A10L]TxIA with wt, P195Q, R185I, and P195Q/R185I α4 subunits (red) and with β2 subunits (green). Overall binding energies are shown in blue. Energies and distances were calculated from 10 to 50 ns.

tion of these mutations also produces improved binding and/or gating efficiency of ACh. Alternatively, this mutation could disturb the expression of correctly folded α4 subunits and result in a reduced α4/β2 subunit ratio, which has been demonstrated to produce α4β2 receptor stoichiometries with high affinity for ACh (Zwart and Vijverberg, 1998). The latter idea is supported by the fact that a decrease in the ratio of injected α4(P195Q)/β RNA resulted in a reduced expression of functional receptors that showed a decreased EC_{50} value for ACh (results not shown).

Homology Models As Prediction Tools. Initial visualization of the receptor-conotoxin complex using a homology model based on the homomeric AChBP (Dutertre et al., 2007) failed to reveal a direct interaction that would prevent α-conotoxin binding (Fig. 4A; Supplemental Fig. 2). However, molecular dynamics and docking studies with [A10L]TxIA on a refined α4β2 homology model based on the *T. marmorata* nAChR demonstrated that the α4Arg185-conotoxin R5 interaction weakens the conotoxin binding, suggesting that this vertebrate receptor, despite the lower resolution of its structure (4 Å compared with 2.7 Å for the AChBP structure), represents a more suitable template to generate rat α4β2 homology models. Nonetheless, a recent crystallization study on a soluble α7/AChBP chimera (Li et al. 2011) that contains loop C of the human α7 receptor with a loop C architecture and side chain positioning similar to those of our AChBP model supports the usefulness of this widely used model. Of interest, loop C of the α7 receptor also contains R and P residues in positions homologous to the α4 subunit. However, the α-conotoxins tested in our study were previously shown to efficiently block the α7 receptor with IC_{50} values of 39 nM ([A10L]TxIA), 100 nM (MII), and 392 nM (TxIA) (Cartier et al., 1996; Dutertre et al., 2007), and several α-conotoxins with even higher potencies at this receptor have been identified. This result is in contrast to the strong effect of these residues in our functional studies and the poor affinity of all identified α-conotoxins at the α4β2 receptor. A possible explanation for this discrepancy could lie in the heteromeric nature of the α4β2 and α3β2 ligand binding sites, which might have a different architecture and for which the heteromeric *T. marmorata* nAChR might provide a better template than the homomeric α7 and AChBP binding sites. In support of this hypothesis, our MD simulations on a *T. marmorata* nAChR-based model reproduced the rank order of potency of the conotoxin [A10L]TxIA on the different α4β2 mutants. A very recent study demonstrated that the homologous positions in the α6 subunit (Ile188 and Thr198) confer selectivity of α-conotoxin BuIA for this subunit (Kim and McIntosh, 2012). A direct interaction between BuIA and Ile188 could not be identified in their model of the complex, and it was suggested that alterations in the loop C structure account for the potency differences of the conotoxin, a conclusion also supported by our MD simulation results.

Design of Optimized α-Conotoxins. α-Conotoxins are important pharmacological tools that can not only discriminate between distinct nicotinic receptor subtypes but also differentiate between nonequivalent binding sites within the same heteromeric receptor (for a review, see Tsetlin et al., 2009). Radioactively labeled or fluorescent α-conotoxins can help receptor localization (Hone et al., 2010; Whiteaker et al., 2008), and α-conotoxins have the potential to be developed into novel drugs (Olivera et al., 2008). So far, natural α-conotoxins with selectivity for the following neuronal nicotinic receptor subtypes have been identified: α3β2 and α6-containing nAChRs (MII), α9α10 nAChRs (RgIA), and α7 and α3β2 nAChRs (ImI) (Ellison et al., 2004, 2008; McIntosh et al., 2004). The subtype selectivity of several α-conotoxins could be further optimized, yielding analogs that are able to differentiate even between closely related nicotinic receptor subtypes. These include α-conotoxins with selectivity for α6-containing nAChRs (MII[S4A;E11A;L15A]), α6β4* nAChRs (BuIA[T5A;P6O]), and α7 nAChRs (ArIB[V11L;V16D]) (Whiteaker et al., 2007; Azam et al., 2008, 2010). Apparently, conotoxins selective for mammalian α4β2 interfaces have not evolved in cone snails or up to now escaped discovery. α4β2-selective α-conotoxins would have the potential not only to differentiate between α4β2 and other nicotinic receptor subtypes but also to help identify multiple α4β2* receptor assemblies, which represents an important task in view of their variety in the central nervous system. In further studies, it is crucial to determine whether α-conotoxins can be designed that are able to bind with high affinity to the α4β2 binding site or whether this requires peptides with different backbone folds.

In conclusion, our study identified an important determinant of subtype selectivity between α3β2 and α4β2 nAChRs

and indicates that α-conotoxins have substantially different binding modes at homomeric α7 and heteromeric α4β2 and α3β2 receptors. This information provides an essential basis and important caveat for further modeling and mutagenesis studies.

Acknowledgments

We thank Christiane Arnold for initial mutant generation and Conny Neblung for technical assistance.

Authorship Contributions

Participated in research design: Dutertre and Nicke.

Conducted experiments: Beissner, Dutertre, Schemm, Danker, Sporning, and Nicke.

Contributed new reagents or analytic tools: Dutertre.

Performed data analysis: Beissner, Dutertre, Schemm, Danker, Grubmüller, and Nicke.

Wrote or contributed to the writing of the manuscript: Dutertre, Schemm, Grubmüller, and Nicke.

References

Azam L, Maskos U, Changeux JP, Dowell CD, Christensen S, De Biasi M, and McIntosh JM (2010) α-Conotoxin BuIA[T5A;P6O]: a novel ligand that discriminates between α6β4 and α6β2 nicotinic acetylcholine receptors and blocks nicotine-stimulated norepinephrine release. *FASEB J* **24:**5113–5123.

Azam L and McIntosh JM (2009) α-Conotoxins as pharmacological probes of nicotinic acetylcholine receptors. *Acta Pharmacol Sin* **30:**771–783.

Azam L, Yoshikami D, and McIntosh JM (2008) Amino acid residues that confer high selectivity of the 6 nicotinic acetylcholine receptor subunit to α-conotoxin MII[S4A,E11A,L15A]. *J Biol Chem* **283:**11625–11632.

Cartier GE, Yoshikami D, Gray WR, Luo S, Olivera BM, and McIntosh JM (1996) A new α-conotoxin which targets α3β2 nicotinic acetylcholine receptors. *J Biol Chem* **271:**7522–7528.

Celie PH, Kasheverov IE, Mordvintsev DY, Hogg RC, van Nierop P, van Elk R, van Rossum-Fikkert SE, Zhmak MN, Bertrand D, Tsetlin V, et al. (2005) Crystal structure of nicotinic acetylcholine receptor homolog AChBP in complex with an α-conotoxin PnIA variant. *Nat Struct Mol Biol* **12:**582–588.

Dowell C, Olivera BM, Garrett JE, Staheli ST, Watkins M, Kuryatov A, Yoshikami D, Lindstrom JM, and McIntosh JM (2003) α-Conotoxin PIA is selective for α6 subunit-containing nicotinic acetylcholine receptors. *J Neurosci* **23:**8445–8452.

Duan Y, Wu C, Chowdhury S, Lee MC, Xiong G, Zhang W, Yang R, Cieplak P, Luo R, Lee T, et al. (2003) A point-charge force field for molecular mechanics simulations of proteins based on condensed-phase quantum mechanical calculations. *J Comput Chem* **24:**1999–2012.

Dutertre S, Nicke A, and Lewis RJ (2005) β2 subunit contribution to 4/7 α-conotoxin binding to the nicotinic acetylcholine receptor. *J Biol Chem* **280:**30460–30468.

Dutertre S, Ulens C, Büttner R, Fish A, van Elk R, Kendel Y, Hopping G, Alewood PF, Schroeder C, Nicke A, et al. (2007) AChBP-targeted α-conotoxin correlates distinct binding orientations with nAChR subtype selectivity. *EMBO J* **26:**3858–3867.

Ellison M, Feng ZP, Park AJ, Zhang X, Olivera BM, McIntosh JM, and Norton RS (2008) α-RgIA, a novel conotoxin that blocks the α9α10 nAChR: structure and identification of key receptor-binding residues. *J Mol Biol* **377:**1216–1227.

Ellison M, Gao F, Wang HL, Sine SM, McIntosh JM, and Olivera BM (2004) α-Conotoxins ImI and ImII target distinct regions of the human α7 nicotinic acetylcholine receptor and distinguish human nicotinic receptor subtypes. *Biochemistry* **43:**16019–16026.

Everhart D, Reiller E, Mirzoian A, McIntosh JM, Malhotra A, and Luetje CW (2003) Identification of residues that confer α-conotoxin-PnIA sensitivity on the α3 subunit of neuronal nicotinic acetylcholine receptors. *J Pharmacol Exp Ther* **306:**664–670.

Gotti C, Clementi F, Fornari A, Gaimarri A, Guiducci S, Manfredi I, Moretti M, Pedrazzi P, Pucci L, and Zoli M (2009) Structural and functional diversity of native brain neuronal nicotinic receptors. *Biochem Pharmacol* **78:**703–711.

Harvey SC, McIntosh JM, Cartier GE, Maddox FN, and Luetje CW (1997) Determinants of specificity for α-conotoxin MII on α3β2 neuronal nicotinic receptors. *Mol Pharmacol* **51:**336–342.

Hess B, Kutzner C, van der Spoel D, and Lindahl E (2008) GROMACS 4: algorithms for highly efficient, load-balanced, and scalable molecular simulation. *J Chem Theory Comput* **4:**435–447.

Hibbs RE and Gouaux E (2011) Principles of activation and permeation in an anion-selective Cys-loop receptor. *Nature* **474:**54–60.

Hone AJ, Whiteaker P, Mohn JL, Jacob MH, and McIntosh JM (2010) Alexa Fluor 546-ArIB[V11L;V16A] is a potent ligand for selectively labeling α7 nicotinic acetylcholine receptors. *J Neurochem* **114:**994–1006.

Kaiser SA, Soliakov L, Harvey SC, Luetje CW, and Wonnacott S (1998) Differential inhibition by α-conotoxin-MII of the nicotinic stimulation of [^{3}H]dopamine release from rat striatal synaptosomes and slices. *J Neurochem* **70:**1069–1076.

Kim HW and McIntosh JM (2012) α6 nAChR subunit residues that confer α-conotoxin BuIA selectivity. *FASEB J* http://dx.doi.org/10.1096/fj.12-204487.

Leisgen C, Kuester M, and Methfessel C (2007) The roboocyte: automated electrophysiology based on *Xenopus* oocytes. *Methods Mol Biol* **403:**87–109.

Li SX, Huang S, Bren N, Noridomi K, Dellisanti CD, Sine SM, and Chen L. (2011) Ligand-binding domain of an α7-nicotinic receptor chimera and its complex with agonist. *Nat Neurosci* **14:**1253–1259.

Loughnan ML, Nicke A, Jones A, Adams DJ, Alewood PF, and Lewis RJ (2004) Chemical and functional identification and characterization of novel sulfated α-conotoxins from the cone snail *Conus anemone*. *J Med Chem* **47:**1234–1241.

Mahoney MW and Jorgensen WL (2000) A five-site model for liquid water and the reproduction of the density anomaly by rigid, nonpolarizable potential functions. *J Chem Phys* **112:**8910–8922.

McIntosh JM, Azam L, Staheli S, Dowell C, Lindstrom JM, Kuryatov A, Garrett JE, Marks MJ, and Whiteaker P (2004) Analogs of α-conotoxin MII are selective for α6-containing nicotinic acetylcholine receptors. *Mol Pharmacol* **65:**944–952.

McIntosh JM, Dowell C, Watkins M, Garrett JE, Yoshikami D, and Olivera BM (2002) α-Conotoxin GIC from *Conus geographus*, a novel peptide antagonist of nicotinic acetylcholine receptors. *J Biol Chem* **277:**33610–33615.

Nicke A, Loughnan ML, Millard EL, Alewood PF, Adams DJ, Daly NL, Craik DJ, and Lewis RJ (2003) Isolation, structure, and activity of GID, a novel α 4/7-conotoxin with an extended N-terminal sequence. *J Biol Chem* **278:**3137–3144.

Nicke A, Wonnacott S, and Lewis RJ (2004) α-Conotoxins as tools for the elucidation of structure and function of neuronal nicotinic acetylcholine receptor subtypes. *Eur J Biochem* **271:**2305–2319.

Olivera BM, Quik M, Vincler M, and McIntosh JM (2008) Subtype-selective conopeptides targeted to nicotinic receptors: concerted discovery and biomedical applications. *Channels (Austin)* **2:**143–152.

Pehl U, Leisgen C, Gampe K, and Guenther E (2004) Automated higher-throughput compound screening on ion channel targets based on the *Xenopus laevis* oocyte expression system. *Assay Drug Dev Technol* **2:**515–524.

Sali A and Blundell TL (1993) Comparative protein modelling by satisfaction of spatial restraints. *J Mol Biol* **234:**779–815.

Taly A, Corringer PJ, Guedin D, Lestage P, and Changeux JP (2009) Nicotinic receptors: allosteric transitions and therapeutic targets in the nervous system. *Nat Rev Drug Discov* **8:**733–750.

Tsetlin V, Utkin Y, and Kasheverov I (2009) Polypeptide and peptide toxins, magnifying lenses for binding sites in nicotinic acetylcholine receptors. *Biochem Pharmacol* **78:**720–731.

Unwin N (2005) Refined structure of the nicotinic acetylcholine receptor at 4A resolution. *J Mol Biol* **346:**967–989.

Whiteaker P, Christensen S, Yoshikami D, Dowell C, Watkins M, Gulyas J, Rivier J, Olivera BM, and McIntosh JM (2007) Discovery, synthesis, and structure activity of a highly selective α7 nicotinic acetylcholine receptor antagonist. *Biochemistry* **46:**6628–6638.

Whiteaker P, Marks MJ, Christensen S, Dowell C, Collins AC, and McIntosh JM (2008) Synthesis and characterization of ^{125}I-conotoxin ArIB[V11L;V16A], a selective α7 nicotinic acetylcholine receptor antagonist. *J Pharmacol Exp Ther* **325:**910–919.

Zwart R and Vijverberg HP (1998) Four pharmacologically distinct subtypes of α4β2 nicotinic acetylcholine receptor expressed in *Xenopus laevis* oocytes. *Mol Pharmacol* **54:**1124–1131.

Address correspondence to: Dr. Annette Nicke, Max Planck Institute for Experimental Medicine, Hermann-Rein-Str. 3, 37075 Göttingen, Germany. E-mail: anicke@gwdg.de